ARTICLE

Microwave Spectrum and Structure of 2-(Trifluoromethyl)pyridine†

Juan Wang, Xiao-long Li, Qian Gou, Gang Feng*

School of Chemistry and Chemical Engineering, Chongqing University, Chongqing 401331, China

(Dated: Received on October 25, 2019; Accepted on November 21, 2019)

The high resolution rotational spectrum of 2-(trifluoromethyl)pyridine in 2−20 GHz was recorded and analyzed. Spectroscopic parameters including rotational constants, nuclear quadrupole coupling constants of ^{14}N as well as the centrifugal distortion constants were determined. The rotational spectra of five mono-substituted ^{13}C and one ^{15}N isotopologues were also measured and assigned in natural abundance. Experimental results complemented by *ab initio* calculations lead to an accurate determination of the skeleton structure. The values of the planar moment inertia P_{cc} were determined to be 44.46 uÅ^2 for all the measured isotopologues, indicating a C_s symmetry of this molecule. The molecular electrostatic surface potential was calculated to illustrate the trifluoromethyl substitution effects on the electron distribution.

Key words: Rotational spectroscopy, Fluorination, Molecular structure, Supersonic expansion, *ab initio* calculation

I. INTRODUCTION

Fluorination of a molecule can significantly alter the properties of the substrate. It can influence the conformational preference, pK_a, membrane permeability, lipophicity and metabolism of molecule [1, 2]. Due to its high electronegativity nature, the incorporation of fluorine into a molecule might also provide an additional non-covalent interaction site, *e.g.*, as the hydrogen bonding acceptor [3, 4]. The structural change upon fluorination can be accurately analysed by means of structural determination from microwave spectroscopy. Therefore, studies of model molecules with different kinds of fluorine bearing functional groups will allow to estimate the fluorination effects in different systems to be quantified.

Similar to fluorine, the incorporation of trifluoromethyl (CF_3) groups into substrates can also significantly influence their properties [5]. Rotational spectroscopic studies of several phenyl compounds disclosed that trifluoroanisole ($PhOCF_3$) prefers an orthogonal conformation [6], different from the anisole ($PhOCH_3$) where a planar conformation is favored [7], suggesting a remarkable perturbation to the conformational behavior by introducing a -CF_3 group into the substances. The -CF_3 substitution effect also determines the different conformational preferences between thioanisole ($PhSCH_3$) and trifluorothioanisole ($PhSCF_3$) [8, 9].

Pyridine (PY) and its derivatives are interesting substrates to model the fluorination effect. Indeed, investigations of mono-fluorinated pyridines [10] demonstrate that fluorination at the *ortho* position of the PY ring has large influence on the electronic structure. The fluorination effect on PY ring was further proven to be more pronounced deviation in difluoropyridines [11], depending on the fluorinated position and the degree of fluorination. The bonding model with hyperconjugation theory and the experimental results demonstrates that fluorine can donate electron density into the π cloud of PY. It might be interesting to study fluorine substitutions away from the ring, starting with a -CF_3 substitution on pyridine. In this study, 2-(trifluoromethyl)pyridine (2TFPY) was investigated by using pulsed jet Fourier transform microwave spectroscopy. The experimental results were complemented by *ab initio* calculations performed at different levels of theory.

II. METHODS

A. Experiments

2TFPY (∼98%) was obtained commercially and used directly for collecting its rotational spectrum. 2TFPY was preserved in a reservoir (∼300 K) coupled in the gas-pipeline. The supersonic expansion was generated by expanding a gas mixture (with Argon as the carrier gas, ∼0.1 MPa) into the Fabry-Pérot cavity using a Series 9 General Valve (0.5 mm). The rotational spectrum was recorded by using a pulsed supersonic-jet Fourier-transform microwave spectrometer with coaxially oriented beam-resonator (COBRA) [12] setup. The frequency range of the spectrometer is 2−20 GHz. The

†Part of the special topic on "The 3rd Asian Workshop on Molecular Spectroscopy".

*Author to whom correspondence should be addressed. E-mail: fengg@cqu.edu.cn

FTMW++ set of programs is used to operate the spectrometer [13, 14]. The spectral signal was recorded in the time-domain with 8×10^3 data points at 100 ns sample intervals. The time-domain signal was then Fourier transformed and converted into the frequency domain. The Doppler effect splits the rotational transition into doublets due to the COBRA setup. The arithmetic means of the two Doppler components is calculated as the rest transition frequency.

B. Theoretical calculations

The Gaussian 16 suite of programs was used for all the calculations [15]. Full geometry optimizations were performed at the B3LYP/aug-cc-pVTZ and the MP2/6-311++G(2d,2p) level of theory. Harmonic frequency analysis was carried out to obtain the zero-point vibrational energy and to derive the quartic centrifugal distortion constants. The molecular electrostatic surface potentials (ESP) of 2TFPY, 2-fluoropyridine (2FPY), 2-methylpyridine (2MPY) and PY were calculated at the B3LYP/aug-cc-pVTZ level of theory.

III. RESULTS

Table I reports the rotational constants (A, B, and C), the nuclear quadrupole coupling constants of ^{14}N (χ_{aa} and $\chi_{bb}-\chi_{cc}$), the electric dipole moment components (μ_a, μ_b, and μ_c), and the centrifugal distortion constants (D_J, D_{JK}, D_K, d_1 and d_2) of 2TFPY while the structure, the principal axes of inertia, and the atomic labels are shown in FIG. 1. The B3LYP/aug-cc-pVTZ and MP2/6-311++G(2d,2p) levels of theory predict close values of spectroscopic parameters for 2TFPY. The values of the dipole moments μ_a and μ_b are calculated to be 4.0 and 1.8 D respectively, suggesting that 2TFPY should have a strong μ_a-type transition and a relatively weaker μ_b-type transition in its pure rotational spectrum. Following the theoretical predictions, the μ_a-R-type transitions of 2TFPY were initially searched. The rotational transitions of J=6←5 band with K_a=0 and 1 were identified firstly. The spectrum displays hyperfine splittings, as shown in FIG. 2, arising from the quadrupole coupling of the ^{14}N nucleus. The measurements were then extended to J_{upper}=3−11 with $K_a\leq5$. Several μ_b-type transitions with weaker intensity were also measured.

The measured transitions were analyzed with the SPFIT program [16] using the Watson's Hamiltonian of S-reduction in I^r representation [17]:

$$H = H_R + H_{CD} + H_Q \quad (1)$$

where H_R stands for the rigid rotational term, H_{CD} stands for the centrifugal distortion contributions, and the H_Q represents the term of ^{14}N quadrupole coupling to the overall rotation. The determined spectroscopic parameters are reported in Table I.

In addition, the rotational spectra of the singly substituted isotopologues of ^{13}C and ^{15}N were measured in natural abundance. Since the number of lines in the isotopologue fits is not enough to determine the centrifugal distortion constants and the quadrupole coupling constants, all values of these parameters were fixed at

TABLE I The theoretical spectroscopic parameters of 2TFPY from the B3LYP/aug-cc-pVTZ and MP2/6-311++G(2d,2p) levels of calculations and comparison with the experimental values (Watson's S reduction, I^r representation).

Parameter	B3LYP	MP2	Expt.
A/MHz	2893	2882	2892.5596(2)[a]
B/MHz	972	977	975.3927(1)
C/MHz	835	837	836.8369(1)
χ_{aa}/MHz	−0.59	−0.48	−0.536(4)
$\chi_{bb}-\chi_{cc}$/MHz	−6.95	−6.26	−6.303(8)
$\lvert\mu_a\rvert$/D	4.0	4.0	Strong
$\lvert\mu_b\rvert$/D	1.8	1.9	Weak
$\lvert\mu_c\rvert$/D	0	0	
D_J/kHz	0.06	0.05	0.0542(5)
D_{JK}/kHz	0.06	0.08	0.068(3)
D_K/kHz	0.05	0.04	[0.0][b]
d_1/Hz	−3.52	−3.55	−3.6(4)
d_2/Hz	16.56	11.84	15.6(3)
P_{cc}[c]/uÅ^2	44.69	44.42	44.46
σ[d]/kHz			2.0
N_{lines}[e]			253

[a] Errors are given in parenthesis expressing in units of the last digit.
[b] Fixed at zero in the fit.
[c] The planar moment of inertia $P_{cc}=\sum_i m_i c_i^2$.
[d] Standard deviation of the fit.
[e] Number of lines fitted.

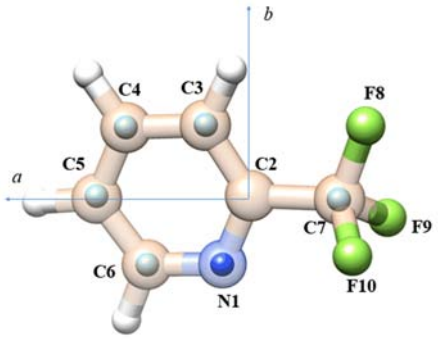

FIG. 1 B3LYP/aug-cc-pVTZ calculated structure, the principal axes of inertia and the atomic labels of 2TFPY. The r_s coordinates of the isotopically substituted atoms are qualitatively shown as blue spheres.

DOI:10.1063/1674-0068/cjcp1910186

TABLE II Spectroscopic parameters determined for the mono-substituted ^{13}C and ^{15}N isotopologues. See FIG.1 for the atomic labels.

	^{15}N1	^{13}C3	^{13}C4	^{13}C5	^{13}C6	^{13}C7
A/MHz	2870.40(2)[a]	2867.43(2)	2870.06(2)	2892.55(2)	2869.05(2)	2892.74(2)
B/MHz	974.3561(3)	973.9704(2)	965.7877(2)	959.9873(2)	967.2762(2)	972.1188(2)
C/MHz	834.2082(2)	833.6728(2)	827.8905(2)	825.4713(2)	828.8961(2)	834.4264(2)
P_{cc}[b]/uÅ^2	44.46	44.46	44.46	44.46	44.46	44.46
σ[c]/kHz	2.2	1.9	1.2	1.5	2.4	0.9
N_{lines}[d]	18	42	42	42	42	42

[a] Errors are given in parenthesis expressing in units of the last digit.
[b] The planar moment of inertia $P_{cc}=\sum_i m_i {c_i}^2$.
[c] Standard deviation of the fit.
[d] Number of lines fitted.

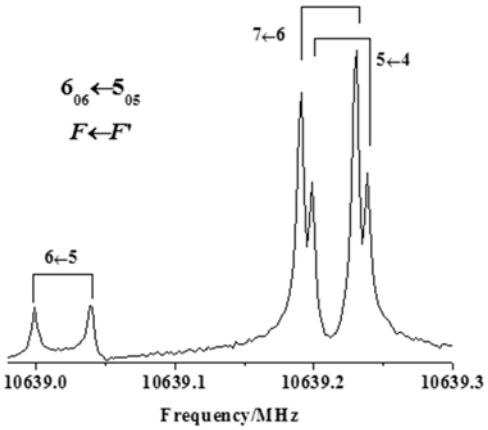

FIG. 2 The hyperfine structure of the recorded $6_{06}\leftarrow5_{05}$ transition of 2TFPY. The hyperfine components (F-F') display as the Doppler doubling (⊓).

TABLE III Comparison of the substituted coordinates (r_s) with the r_e coordinates of 2TFPY.

	r_s		r_e	
	a/Å	b/Å	a/Å	b/Å
N1	±0.746(2)	±1.168(1)	0.763	−1.161
C2	/[a]	/[a]	0.184	0.037
C3	0.871(2)	±1.242(1)	0.882	1.236
C4	±2.270(1)	±1.182(1)	2.271	1.178
C5	±2.888(1)	±0.022(71)	2.890	−0.063
C6	±2.085(1)	±1.207(1)	2.092	−1.204
C7	±1.325(1)	0[b]	−1.334	0.007

[a] The unavailable coordinates. The corresponding *ab initio* values are used in structural calculation.
[b] Imaginary value, fixed at zero.

those values reported in Table I for the parent species. The rotational spectrum of the ^{15}N isotopologue is free from the quadrupole coupling splitting because the ^{15}N nuclear spin quantum number is 1/2. To analyse the spectrum of ^{15}N species, the H_Q term of Eq.(1) is removed from the Hamiltonian. As indicated in FIG. 1, the C2 atom is near its center of mass, hence its rotational spectrum is mostly overlapped with the parent species and therefore unmeasurable. Table II reports the determined spectroscopic constants for all the substituted isotopologues. The transition frequencies of all the measured isotopologues are present in the supplementary materials.

IV. DISCUSSION

A. Molecular structure

The planar moment of inertia (P_{cc}), presenting the mass distributions out of the *ab* plane, has identical values for the parent and all the singly substituted isotopologues (Tables I and II), suggesting that all those atoms are in the *ab* plane. The rotational constants of the parent and all the singly substituted isotopologues were used to calculate the r_s coordinates of the atoms using the Kraitchman's equations [18] with the corresponding Costain's errors [19]. The obtained r_s coordinates are summarized in Table III which are also included in FIG. 1 represented by blue spheres for the directly visual comparison. The r_e coordinates (B3LYP/aug-cc-PVTZ) match the r_s values quite well. In order to deduce the bond lengths and the valence angles of the whole skeleton (Table IV), the r_e coordinates of C2 were used in the structural calculations. The r_0 structure was reproduced by a least-squares fit taking all sets of rotational constants into account using the STRFIT program [20] to obtain the effective structure of 2TFPY. The determined effective structure is apparently the same as the equilibrium structure calculated at the B3LYP/aug-cc-pVTZ level of theory (Table S8 in supplementary materials).

DOI:10.1063/1674-0068/cjcp1910186

TABLE IV Comparison of r_s-structure and r_e-structure (B3LYP/aug-cc-pVTZ) of PY, 2FPY, and 2TFPY.

	PY		2FPY		2TFPY	
	r_e	r_s[a]	r_e	r_s[a]	r_e	r_s
N1C2/Å	1.333	1.340(2)[b]	1.306	1.310(18)	1.330	1.365[c]
C2C3/Å	1.391	1.390(3)	1.390	1.387(18)	1.388	1.452[c]
C3C4/Å	1.388	1.394(2)	1.385	1.386(11)	1.390	1.398(1)
C4C5/Å	1.388	1.394(2)	1.393	1.40(4)	1.386	1.36(3)
C5C6/Å	1.391	1.390(3)	1.386	1.39(4)	1.392	1.43(3)
C6N1/Å	1.333	1.340(2)	1.338	1.345(6)	1.329	1.339(1)
C7C2/Å					1.518	1.408[c]
∠N1C2C3/°	123.5	123.8(3)	125.8	127(2)	124.0	120.5[c]
∠C2C3C4/°	118.5	118.6(3)	116.6	116.5(16)	117.8	117.9[c]
∠C3C4C5/°	118.6	118.3(2)	119.2	119(4)	118.9	119.5(7)
∠C4C5C6/°	118.5	118.6(3)	118.3	118(4)	118.5	118.7(1)
∠C5C6N1/°	123.5	123.8(3)	123.1	123(4)	123.1	122.4(8)
∠C6N1C2/°	116.9	116.8(2)	117.0	116.0(15)	117.6	118.1[c]

[a] Structural parameters from Ref.[10].
[b] Errors are given in parenthesis expressing in units of the last digit.
[c] r_s structural parameters calculated with the coordinates of the C_2 atom fixed at the theoretical values.

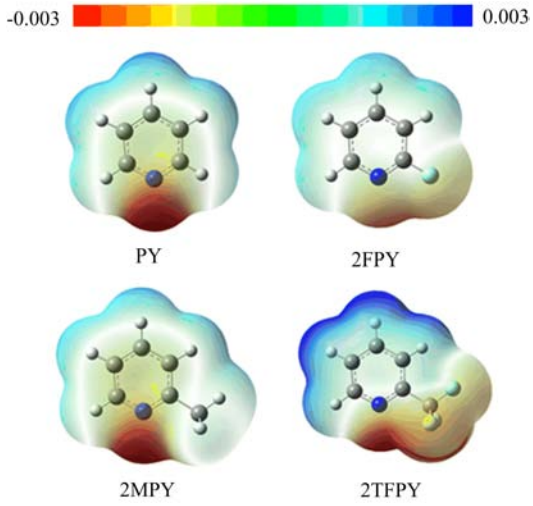

FIG. 3 The MESPs of PY, 2FPY, 2MPY, and 2TFPY. The isosurface was chosen at the 0.0004 electrons/bohr^3.

B. Fluorination effect

In order to illustrate the fluorination effects, the molecular electrostatic surface potentials (ESP) of PY, 2FPY, 2MPY and 2TFPY were calculated (FIG. 3). For all the four molecules, the lone pair of the N atom represents the most negative potential site (red). The substitution of H with fluorine at the *ortho*-position of the pyridine ring induces a decrease of the N atom electron density, where F atom provides an additional negative electron density site. The methyl substation at the *ortho*-position affects the N atom electron density insignificantly but it induces an increase of the pyridine ring electron density. Substitution of -CF_3 at the *ortho*-position noticeably reduces the electron density of the pyridine ring and also the electron density of hydrogen atoms. The N atom and the -CF_3 group represent the negative electron density. The change of electron distribution due to the incorporation of F or -CF_3 group into the pyridine ring can also be reflected by the atomic charge of the N and the C of *ortho*-position. Table V reports the atomic charge of the N and the *ortho*-C atoms from a natural population analysis. The incorporation of the -CF_3 group at the *ortho*-position of the pyridine weakens the nucleophilicity of the N atom distinctly. F substitution at the *ortho*-position enhances the electropositivity of the *ortho*-C atom.

TABLE V Comparison of NPA charge distributions of PY, 2FPY, 2MPY, and 2TFPY.

	PY	2FPY	2MPY	2TFPY
N/e	−0.426	−0.451	−0.443	−0.397
C2/e	0.043	0.591	0.213	0.092
C6/e	0.043	0.057	0.054	0.054

V. CONCLUSION

The rotational spectra of 2-(trifluoromethyl)pyridine in 2−20 GHz and its six mono-substituted isotopologues were measured and assigned. The structure of the heavy atoms skeleton was experimentally determined. The analysis of the experimental rotational constants suggests that P_{cc} values of the parent and all the measured mono-substituted isotopologues are 44.46 uÅ^2, indicat-

DOI:10.1063/1674-0068/cjcp1910186

ing a C_s symmetry of the molecule. The incorporation of -CF_3 group into the pyridine ring at the *ortho*-position reduces the electron distribution of the π electron of the pyridine ring and the N atom.

Supplementary materials: The measured transition frequencies for 2TFMPY (Tables S1−S7) and the effective structure (r_0) of 2TFMPY (Table S7) are given.

VI. ACKNOWLEDGMENTS

This work was supported by the National Natural Science Foundation of China (No.21703021 and No.U1931104), Chongqing University under the program of the Foundation of 100 Young, Fundamental and Frontier Research Fund of Chongqing (No.cstc2017jcyjAX0068 and No.cstc2018jcyjAX0050), and Venture & Innovation Support Program for Chongqing Overseas Returns (No.cx2018064).

[1] F. Leroux, P. Jeschke, and M. Schlosser, Chem. Rev. **105**, 827 (2005).
[2] C. Thiehoff, Y. P. Rey, and R. Gilmour, Isr. J. Chem. **57**, 92 (2017).
[3] D. O. Hagan, Chem. Soc. Rev. **37**, 308 (2008).
[4] Hans-Jörg Schneider, Chem. Sci. **3**, 1381 (2012).
[5] R. Berger, G. Resnati, P. Metrangolo, E. Weber, and J. Huliger, Chem. Soc. Rev. **40**, 3496 (2011).
[6] M. Onda, A. Toda, S. Mori, and I. Yamaguchi, J. Mol. Struct. **144**, 47 (1986).
[7] L. Kang, S. E. Novick, Q. Gou, L. Spada, M. Vallejo-Lopez, and W. Caminati, J. Mol. Spectrosc. **297**, 32 (2014).
[8] B. Velino, S. Melandri, W. Caminati, and P. G. Favero, Gazz. Chim. It. **125**, 373 (1995).
[9] Y. Jin, J. Wang, Q. Gou, Z. Xia, and G. Feng, J. Mol. Struct. **1156**, 230 (2018).
[10] C. W. van Dijk, M. Sun, and J. van Wijngaarden, J. Phys. Chem. A **116**, 4082 (2012).
[11] C. W. van Dijk, M. Sun, and J. van Wijngaarden, J. Mol. Spectrosc. **280**, 34 (2012).
[12] J. U. Grabow, W. Stahl, and H. Dreizler, Rev. Sci. Instrum. **67**, 4072 (1996).
[13] T. J. Balle and W. H. Flygare, Rev. Sci. Instrum. **52**, 33 (1981).
[14] J. U. Grabow, Q. Gou, and G. Feng, *A Highly-Integrated Supersonic-Jet Fourier Transform Microwave Spectrometer. 72nd International Symposium on Molecular Spectroscopy, TH03*, Champaign-Urbana: International Symposium on Molecular Spectroscopy, (2017).
[15] M. J. Frisch, G. W. Trucks, H. B. Schlegel, G. E. Scuseria, M. A. Robb, J. R. Cheeseman, G. Scalmani, V. Barone, G. A. Petersson, H. Nakatsuji, X. Li, M. Caricato, A. V. Marenich, J. Bloino, B. G. Janesko, R. Gomperts, B. Mennucci, H. P. Hratchian, J. V. Ortiz, A. F. Izmaylov, J. L. Sonnenberg, D. Williams-Young, F. Ding, F. Lipparini, F. Egidi, J. Goings, B. Peng, A. Petrone, T. Henderson, D. Ranasinghe, V. G. Zakrzewski, J. Gao, N. Rega, G. Zheng, W. Liang, M. Hada, M. Ehara, K. Toyota, R. Fukuda, J. Hasegawa, M. Ishida, T. Nakajima, Y. Honda, O. Kitao, H. Nakai, T. Vreven, K. Throssell, J. A. Montgomery Jr., J. E. Peralta, F. Ogliaro, M. J. Bearpark, J. J. Heyd, E. N. Brothers, K. N. Kudin, V. N. Staroverov, T. A. Keith, R. Kobayashi, J. Normand, K. Raghavachari, A. P. Rendell, J. C. Burant, S. S. Iyengar, J. Tomasi, M. Cossi, J. M. Millam, M. Klene, C. Adamo, R. Cammi, J. W. Ochterski, R. L. Martin, K. Morokuma, O. Farkas, J. B. Foresman, and D. J. Fox, *Gaussian 16, Revision A.03*, Wallingford CT: Gaussian Inc., (2016).
[16] H. M. Pickett, J. Mol. Spectrosc. **148**, 371 (1991).
[17] J. K. G. Watson, *in Vibrational Spectra and Structure*, Vol.6, J. R. Durig Ed., New York/Amsterdam: Elsevier, 1, (1977).
[18] J. Kraitchman, Am. J. Phys. **211**, 17 (953).
[19] C. Costain, J. Chem. Phys. **29**, 864 (1958).
[20] Z. Kisiel, J. Mol. Spectrosc. **218**, 58 (2003).

DOI:10.1063/1674-0068/cjcp1910186